Conductance of a Cobalt(II) Terpyridine Complex Based Molecular Transistor: A Computational Analysis†

Trilisa M. Perrine and Barry D. Dunietz*

The University of Michigan, Ann Arbor, Michigan 48109

Received: August 7, 2007; In Final Form: October 11, 2007

A recent experiment, in which a molecular transistor based on the coordination chemistry of cobalt(II) and organic self-assembled monolayers is formed by means of self-aligned lithography,[2] is analyzed with a computational approach. The calculations reveal that a complex involving two cobalt(II) ions bridged by acetate ions can effectively span the nanogap. This bridged complex is shown to be both more flexible and more conductive than the alternative structure involving a single cobalt(II) ion. The single cobalt(II) ion complex is the more stable structure in a nonconfined environment (i.e., in solution) but is found to be less effective at connecting the leads of the fabricated gap and is less likely to result in a conductive device.

1. Introduction

A central goal of nanoscience research is the further miniaturization of electronic devices. The fabrication of metallic gaps which enclose single molecules is a core challenge in the field. Recently, molecular transistors with specific chemical reactivity were fabricated using self-aligned lithography and self-assembled monolayers (SAMs).[1,2] In the experiment, metallic electrodes are produced with nanoscale separations, and monolayers of thiol-functionalized terpyridine-terminated molecules (4-(2,2′:6′,2″-terpyridine)benzenethiol) are then assembled on each of the two aligned electrodes. Figure 1 illustrates this arrangement and the subsequent reaction. A molecular junction is produced by introducing a linking component (cobalt(II) acetate) to the system. This reaction results in a connection between the two SAMs, and thus a molecular junction between the two electrodes.

The coordination chemistry of cobalt(II) with 2,2′:6′,2″-terpyridine (terpy) based ligands has been widely studied.[3−6] Bis-terpyridine complexes, in which two terpy-based ligands are bound to the metal ion, are readily produced.[7,8] Mono-terpyridine complexes, involving only one terpy ligand, have also been isolated.[4,5,9,10] These complexes are well-known for their use in molecular devices.[11]

In the lithography experiment, non-negligible current is only measured after the $Co(OAc)_2$ is allowed to react with the SAMs, where an increase of 3 orders of magnitude is observed.[1] This formation of a conductive molecular junction is reversible by the addition of EDTA, which extracts the linking unit and, therefore, breaks the junction.[2] Here we employ computational models to provide a molecular scale description of the conductance structure−function relations of these devices.

2. Computational Details

Optimized geometries for the molecular systems are first obtained from DFT calculations by employing QChem 3.1.[12] In all computations, the B3LYP[13,14] functional and the LANL2DZ[15] basis set are utilized. The organic molecules are bonded through thiols to ideal flat Pt(111) surfaces containing 12 atoms with Pt−Pt bond lengths of 2.775 Å. The platinum surfaces are constrained to remain parallel; however, the distance between the surfaces is allowed to relax. The bulk platinum is represented by addition of layers of six platinum atoms to the Pt(111) surface.

Figure 1. Reaction scheme utilized in the experiment.[1,2] Two monolayers of 4-(2,2′:6′,2″-terpyridine)benzenethiol are self-assembled onto platinum surfaces formed by self-aligned lithography. Cobalt(II) acetate is then added, and the system is allowed to react.

Single point energies are computed for these extended models and are analyzed using the Green's function (GF) formalism, as outlined by others, to calculate the electron transmission functions.[16−22] We follow the scattering-based picture of molecular conductance[23−25] to obtain the transmission and current. These calculations include a representation of the semi-infinite bulk by efficiently solving a tight-binding (TB) model of the bulk at every energy, where the surface and bulk GFs are solved for iteratively and simultaneously.[26,27] The TB parameters are extracted from the electronic structure calculations described above.

3. Results and Discussion

Experimentally, the molecular devices are chemically synthesized within the self-aligned nanogaps, *in situ*.[1] In this procedure the organic portions of the device are first bound to the metallic leads, and then the linking metal ion is added. This imposes certain constraints on the system that are not present when reacting the organic molecules with the same ionic reagent outside of the nanogaps, *ex situ*. It is, therefore, important to explore the effect of such constraints on the geometry and function of the molecular devices. To that end, various models of the molecular device are used to determine the possibility for current flow through the system. These models, which include the surface binding Pt atoms, are shown in Figure 2.

First, the bis complex illustrated in Figure 2a is considered. This complex contains a single cobalt(II) ion and will be referred

† Part of the "William A. Lester, Jr., Festschrift".

10.1021/jp076313z CCC: $40.75
Published on Web 11/29/2007

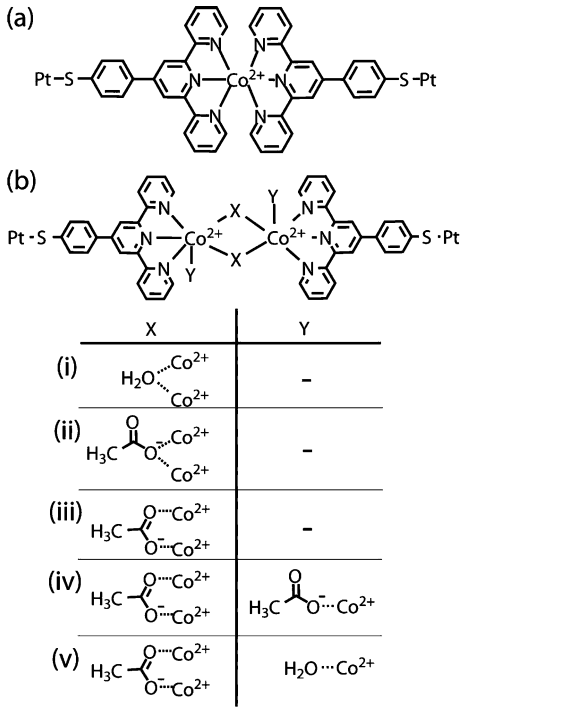

Figure 2. Systems potentially formed *in situ* during the experiment [(4-(2,2′:6′,2″-terpyridine)phenylthio)platinum is abbreviated as Pt-S-ph-terpy.] (a) Bis(Pt-S-ph-terpy)cobalt(+2) [Mono-Co^{2+}].[28] (b) Various ligation schemes are considered where X and Y represent the ligands shown: (i) Bis(μ-aqua)bis((Pt-S-ph-terpy)cobalt)(+4) [**2bi**]; (ii) bis(μ-acetato-κO)bis((Pt-S-ph-terpy)cobalt)(+2) [**2bii**]; (iii) bis(μ-acetato-κ^2O,O′)bis((Pt-S-ph-terpy)cobalt)(+2) [**Di-Co**$^{2+}$];[28] (iv) bis(μ-acetato-κ^2O,O′)bis(acetato(Pt-S-ph-terpy)cobalt) [**2biv**]; (v) bis(μ-acetato-κ^2O,O′)bis(aqua(Pt-S-ph-terpy)cobalt)(+2) [**2bv**].

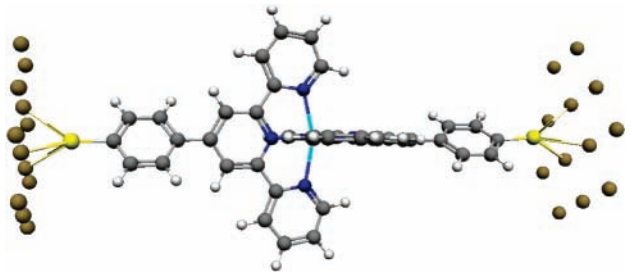

Figure 3. 3D molecular model of Mono-Co^{2+}.

to as Mono-Co^{2+} hereafter. Reactions in a solution of Co^{2+} ions and terpyridine-based molecules (similar to the reaction performed in the nanogaps) yield bis complexes, with a 1:2 ratio of cobalt(II) ion to the terpyridine-based ligand, even at relatively high metal ion concentrations. It has been shown that the bis-terpyridine complexes with cobalt(II) are significantly more stable than the 1:1 complexes.[6−8] The optimized structure of Mono-Co^{2+} is illustrated in Figure 3.

The computed optimized structure is partially constrained by maintaining the planarity of the Pt layers and the Pt−Pt bond lengths, and by keeping the two surfaces parallel to each other. The distance between the surfaces is allowed to relax; for Mono-Co^{2+}, this optimized distance is 25.74 Å. The distance between the platinum leads produced by the self-aligned lithography procedure is roughly estimated to be 30 Å.[1] Our calculations demonstrate that Mono-Co^{2+} cannot stretch to 30 Å. However, the precision of the nanogap fabrication process is unclear, and the range of fabricated distances is difficult to determine. Therefore, it is still possible that this shorter molecule may span the fabricated gap if the width is, in actuality, smaller than 30 Å.

We now highlight another important geometric constraint, which is a direct consequence of the experimental procedure. In the fabrication process, the monolayers are formed on the platinum surfaces *before* introduction of the cobalt(II) ion. In this arrangement, the terpyridine units are constrained by the thiol platinum bonds and are not free to orient themselves optimally with respect to each other to bind the Co^{2+} ion. Due to this tethering effect, and the nanogap width consideration, alternate ligation schemes are considered below.

The experimental data provide further indication that an alternate ligation scheme may be responsible for the conductive state. In a control experiment, the terpyridine-based organic molecules were reacted with cobalt(II) acetate *ex situ* and the product of this reaciton was then exposed to the platinum nanogaps. In this experiment, no conducting devices were detected.[2] Our calculations provide an explanation for this observation as well. The Mono-Co^{2+} bis-terpyridine compound is the most stable of the complexes considered by approximately 20 kcal/mol in a nonconfined environment where the platinum surfaces are not considered. These results along with previous experimental evidence[6−8] indicate, therefore, that it is the bis-terpyridine complex (Mono-Co^{2+}) that is produced *ex situ* and subsequently introduced into the nanogaps in the control experiment. However, as noted above, this Mono-Co^{2+} complex is not long enough to effectively span a 30 Å gap. Furthermore, even in the situation where the gap is short enough to be linked by this structure, our calculations, as discussed in detail below, indicate that only low transmission is expected through this structure.

Bis complexes, such as Mono-Co^{2+}, can yield a related mono-terpyridine complex of cobalt(II) by heating until one terpyridine ligand dissociates from the ion.[4,9] In solution, the resulting low coordination complex, with a single tridentate terpyridine ligand, may additionally bind to two or three other available ligands. The cobalt(II) ion in a bis-terpyridine complex is 6 coordinated; the mono-terpyridine compounds contain either 5 or 6 coordinated metal centers.[5,9]

These mono-terpyridine complexes, however, would not be able to bond simultaneously to both electrodes. Therefore, we consider the possibility of bridging (μ-type) ligands, which can result in complexes that extend from one platinum lead to the other. These structures have the potential to transform the isolated mono-terpyridine structures into molecular wires, and this bridged structure formation may serve to explain the experimentally observed jump in transmission upon addition of the $Co(OAc)_2$ linking agent. The additional ligands, which are available at the experimental conditions, are acetate and water. These ligands can directly participate in the complexation process; therefore, several ligation schemes are considered that would connect the two SAMs through these bridging ligands. These schemes are shown in Figure 2b.

Geometry optimizations of the systems are first performed without the platinum surfaces to determine the relative energetics of the complexes. We find that the use of water ligands (Figure 2bi) does not result in a stable bridged complex, as the two monomeric halves are repelled. The acetate ion is another potential bridging ligand and is considered next.

Two possibilities for bridging by the acetate ion are explored and are shown in Figure 2bii and 2biii. An acetate ion may bridge the cobalt(II) ions by use of one oxygen atom (**2bii**) or through the use of both of its available oxygen atoms (**2biii**). The **2biii** complex is found to be stable, whereas a **2bii** geometry optimization resulted in a **2biii** conformer. The **2biii**-based systems in which additional ligands are bound to each of the

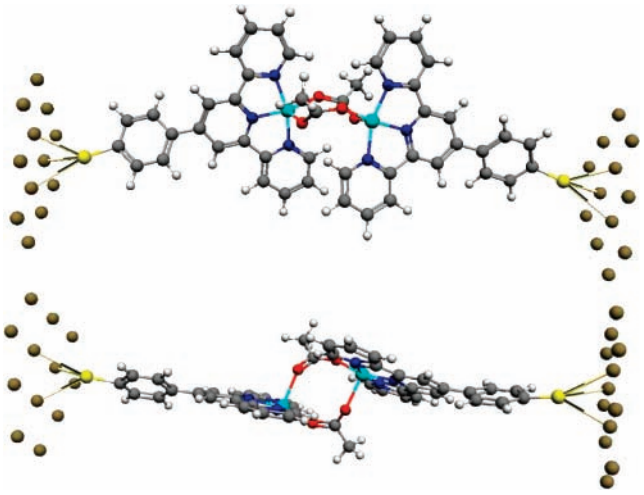

Figure 4. Two 3D views of Di-Co^{2+}.

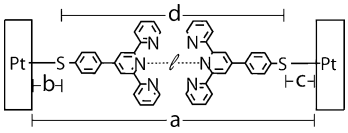

Figure 5. Diagram defining the parameters listed in Table 1. *l* represents the linking scheme.

metal ions (acetate or water as the Y ligands in Figure 2biv and 2bv) are computed to be less thermodynamically stable than the **2biii** system in which each Co^{2+} ion is 5 coordinate. This identified most stable bridged system involving two cobalt(II) ions will be referred to as Di-Co^{2+} hereafter. The Co−Co distance in the Di-Co^{2+} structure is 4.6 Å.[28]

The Di-Co^{2+} system is subsequently optimized between two parallel platinum surfaces. The relaxed Pt−Pt distance is 29.80 Å. This is in good agreement with the experimental estimate of the nanogap. A molecular model of this geometry is shown in Figure 4 from two complementary perspectives to illustrate its geometry clearly. An important feature of this structure is the parallel alignment of the conjugation planes of the terpy ligands, in contrast to the perpendicular alignment of these planes in the Mono-Co^{2+} system.

Because the molecular wires are formed *in situ* experimentally, a system that is flexible and stable under various platinum surface separations is advantageous to enhance the fabrication of conducting junctions. This flexibility allows for the successful formation of junctions under a wider range of nanogap widths, where the junction formation is less dependent on the relative orientation of the molecules in the opposing SAMs. The flexibility of the Mono-Co^{2+} and Di-Co^{2+} geometries is, therefore, examined in detail next.

Geometry optimizations are performed at several constrained distances between the Pt surfaces for both Mono-Co^{2+} and Di-Co^{2+}. Four parameters, which are representative of the overall flexibility of the considered complexes, are labeled in Figure 5 and listed in Table 1: *a* is the constrained distance between the platinum surfaces, *b* and *c* are the distances between each platinum surface and the nearest sulfur atom, and *d* is the distance between the two sulfur atoms. Stable devices are likely to form over a wider range of values of the *a* parameter for Di-Co^{2+} than for Mono-Co^{2+}.

It is, therefore, evident from the optimized geometries that Di-Co^{2+} is a more flexible complex than Mono-Co^{2+} and can form a molecular junction between platinum surfaces within a larger range of surface separations. More specifically, stable

TABLE 1: Distances in the Optimized Structures of Mono-Co^{2+} and Di-Co^{2+} (Figure 5)[a]

a (Å)	*b* (Å)	*c* (Å)	*d* (Å)
	Mono-Co^{2+}		
25.0	2.13	2.02	21.12
no Pt			21.70
25.7[b]	2.16	2.03	21.55
26.0	2.40	2.29	21.33
27.0	*3.24*	2.30	21.51
28.0	*3.86*	2.44	21.70
29.0	*5.29*	2.19	21.60
30.0	*6.28*	2.28	21.45
	Di-Co^{2+}		
no Pt			23.82
27.0	2.13	2.07	22.80
28.0	2.20	2.10	23.70
29.0	2.38	2.32	24.31
29.8[b]	2.41	2.49	24.90
30.0	2.46	2.44	25.10
31.0	2.43	2.55	26.05
32.0	*3.00*	*3.18*	25.86
33.0	*4.21*	*4.32*	24.56

[a] *a* is the distance between the platinum surfaces.*b* and *c* are the distances between each platinum surface and the nearest sulfur atom. *d* is the distance between the two sulfur atoms. The S−S distance for the system with no Pt included (S−H terminated molecule) is also given as a reference. Values in italics are longer than a typical S−Pt bond length. [b] The relaxed platinum surface separations for each system.

junctions are formed for Di-Co^{2+} with $a = 27.0-31.0$ Å, and Mono-Co^{2+} forms junctions in a much smaller range of *a* (from 25.0 to 26.0 Å). Furthermore, the energy penalty throughout the narrower range of *a* distances for Mono-Co^{2+} (16.7 kcal/mol) is an order of magnitude greater than it is for Di-Co^{2+} (1.8 kcal/mol). In addition, an examination of the values of *d* for the various optimizations also demonstrates that Di-Co^{2+} is more flexible than Mono-Co^{2+}. The distance between the sulfur atoms changes from 22.80 to 26.05 Å at the extremes for Di-Co^{2+}; the system without any platinum surfaces has a value of $d = 23.82$ Å. For Mono-Co^{2+} the distance between the sulfur atoms (*d*) at various Pt−Pt separations differs very little (less than 0.6 Å) from the value of the complex without Pt, where $d = 21.70$ Å. This demonstrated flexibility of the Di-Co^{2+} complex suggests a greater ability to form a molecular link under the confining circumstances of a nanogap. The conductive properties of Di-Co^{2+} are considered next and are compared with those of Mono-Co^{2+}.

The transmission through Mono-Co^{2+} and Di-Co^{2+} at their optimal Pt−Pt distances and Di-Co^{2+} at a constrained 30.0 Å Pt−Pt gap width is computed. The transmission functions are shown in Figure 6. The current computed for each of the systems is plotted in Figure 7. Most importantly, the Mono-Co^{2+} system is a significantly poorer conductor than the bridged system, with almost negligible transmission occurring near the Fermi level (E_f). Di-Co^{2+}, on the other hand, shows appreciable transmission at approximately 1 eV above E_f. This transmission results in current through Di-Co^{2+} that is 7−13 times that through Mono-Co^{2+}, depending on the distance between the electrodes.

We now discuss the distance dependence of the transmission of the two systems. The energetically optimized distance between the platinum layers for Di-Co^{2+} is found to be 29.80 Å. The gap between the platinum surfaces in the experiment is approximately 30 Å, where the acetate bridged complex is likely to form. Furthermore, the transmission and current (Figures 6 and 7) indicate that a Di-Co^{2+} molecular device constrained to 30.0 Å is an even better conductor than the relaxed Di-Co^{2+} device. Both the constrained and relaxed Di-Co^{2+} systems are

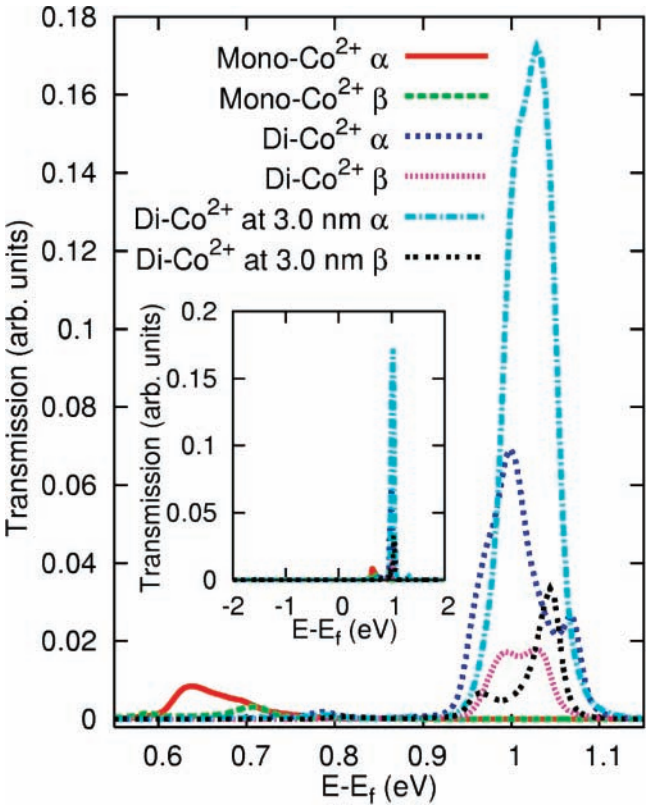

Figure 6. Transmission through Mono-Co^{2+}, Di-Co^{2+}, and Di-Co^{2+} constrained to a 3.0 nm Pt−Pt layer distance versus the difference in energy from the Fermi energy [E_f] of the leads (in eV). The α and β channels are plotted separately. The inset shows a wider energy range of the transmission for the same systems.

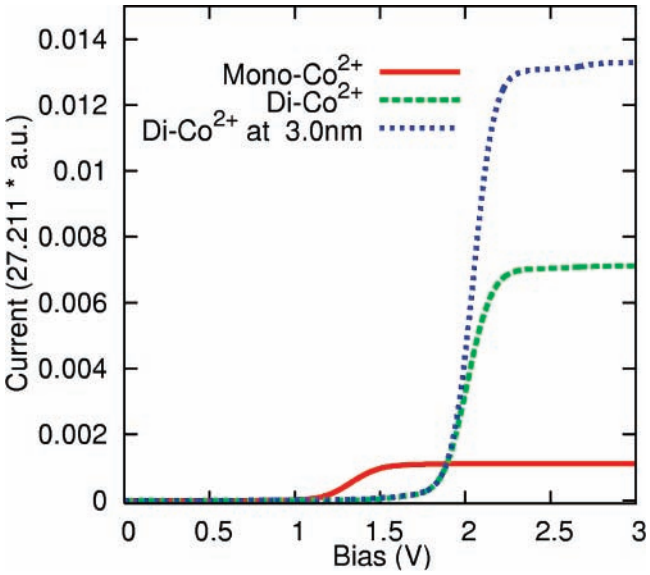

Figure 7. Current through Mono-Co^{2+}, Di-Co^{2+}, and Di-Co^{2+} constrained to a 3.0 nm Pt−Pt layer distance versus applied bias. Currents through the α and β channels are summed.

considerably better conductors than Mono-Co^{2+}. Despite the fact that Mono-Co^{2+} is less flexible than Di-Co^{2+}, for completeness, we have also computed the transmission of a slightly stretched Mono-Co^{2+} system (26.0 Å). This system displays even less transmission than the relaxed Mono-Co^{2+} system.

The difference in the transmission of the systems is further analyzed by focusing on the electronic structure of each complex. The transmission for each of the systems within 2 eV of E_f is exclusively through unoccupied orbitals. Molecular

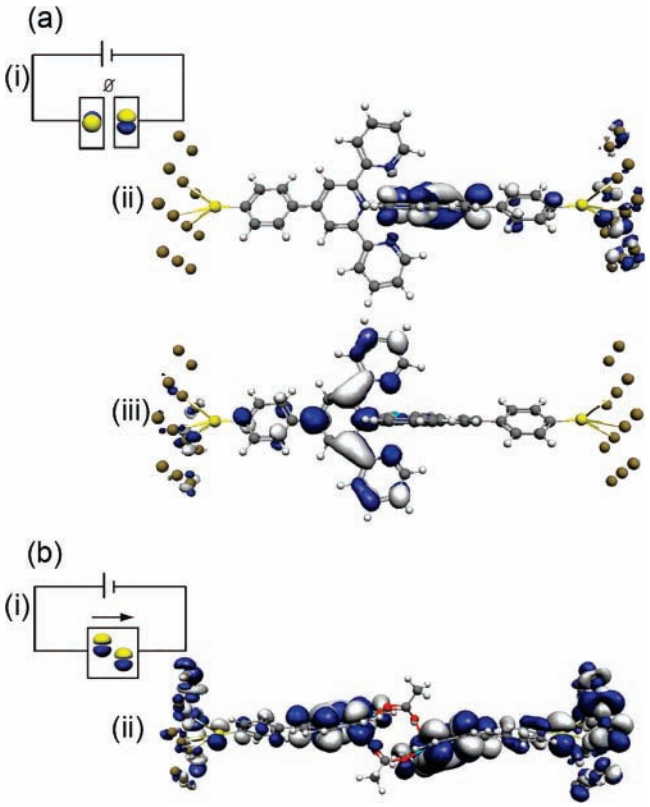

Figure 8. (a) (i) Incomplete circuit formed by Mono-Co^{2+} spanning a nanogap. Representative molecular orbitals of Mono-Co^{2+} that lie at (ii) +0.572 and (ii) +0.708 eV from E_f. (b) (i) Complete circuit formed by Di-Co^{2+} spanning a nanogap. (ii) Representative molecular orbital of Di-Co^{2+}.

orbitals responsible for the slight transmission through Mono-Co^{2+} are plotted in Figure 8a. The small magnitude of the transmission results from the nature of the ligands' π molecular orbitals and their interactions across the Co^{2+} center. The π systems of the organic portions of the complex interact with the cobalt(II) ion center through the d orbitals of the ion. The two halves of the complex are, however, oriented 90° from each other and thus interact with orthogonal d orbitals on the cobalt ion. This bonding scheme to the metal center does not allow for the π system on one-half of the complex to interact significantly with the π system on the other half. The resulting orbitals are each, therefore, localized on one side of the complex. Thus, very little transmission is permitted through this complex.

In contrast, the organic portions of Di-Co^{2+} are aligned in such a way that there is significant interaction between the π molecular orbitals on one-half of the complex, with the π orbitals on the other half of the complex. Figure 8b illustrates this with a representative molecular orbital of Di-Co^{2+}. The acetate ions, therefore, play a significant role in the ability of this system to transmit, as they allow for the formation of a bridged complex and the delocalization of the π molecular orbitals across both halves of the complex. This results in appreciable transmission and conductance through the system as shown in Figure 6 and 7. The further increased transmission and current through the Di-Co^{2+} at 30.0 Å system is related to improved interaction of the π systems on the two terpyridine ligands.

The π interaction in Di-Co^{2+} results in a limited π stacking arrangement of the two conjugated systems. The $\pi-\pi$ stacking interaction is between two of the pyridine rings (one on each of the terpyridine ligands) for Di-Co^{2+}. This attractive interaction is enhanced at the constrained 30.0 Å distance relative to either the relaxed Pt−Pt distance or even the optimized system without

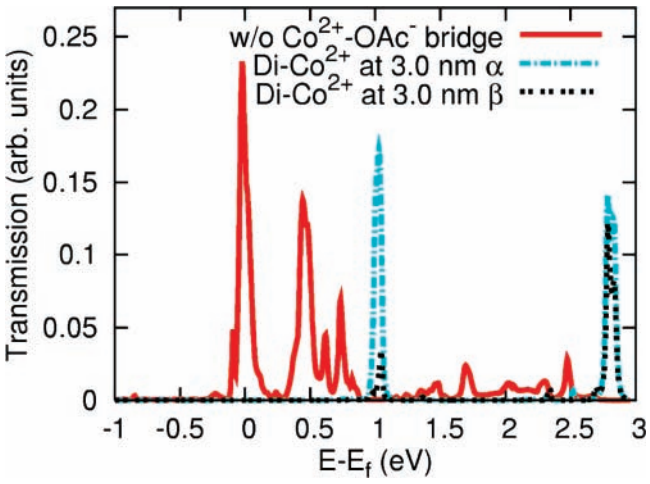

Figure 9. Transmission through Di-Co^{2+} constrained to a 3.0 nm Pt−Pt layer distance and the same geometry without the cobalt(II) and acetate ions bridging the terpyridine units versus the difference in energy from the Fermi energy [E_f] of the leads (in eV). The α and β channels are plotted separately for Di-Co^{2+} constrained to a 3.0 nm Pt−Pt layer distance, and only the α channel is shown for the other system because it is a singlet and the α and β channels are identical.

the platinum leads. This augmented $\pi-\pi$ stacking increases the delocalization of the π molecular orbitals across the system and thus results in improved transmission. The Di-Co^{2+} system with the greater $\pi-\pi$ stacking is not energetically the most favorable, as $\pi-\pi$ stacking is a weak interaction with binding energies on the order of only a few kcal/mol.[29]

As discussed above, the metal ions play a vital role in the formation of the bridged complex, Di-Co^{2+}. We now consider the effect they have on the transmission. The presence of metal ions in complex-based molecular wires can have a direct effect on the conductance of a molecular junction in various ways.[21,30,31] Metal centers have specifically been shown to play a crucial role in facilitating transmission through some systems.[31,32] To determine the role that the metal ions play in the transmission through Di-Co^{2+}, a model was considered on the basis of the constrained 30.0 Å Di-Co^{2+} geometry. The two cobalt(II) and bridging acetate ions were removed from the geometry, and transmission for the remaining terpyridine based molecules was computed. This transmission is plotted in Figure 9 beside the transmission of the full Di-Co^{2+} constrained to 30.0 Å system. This model is clearly artificial because the geometry is not allowed to relax; however, it serves to illustrate the relative effects of the $\pi-\pi$ stacking and the metal ions on the transmission. The transmission through the system without the metal ions is interestingly enhanced over the Di-Co^{2+} system, which includes the metals and bridging acetates.

The metal and bridging acetate ions are critical to the structure of Di-Co^{2+}; however, they have a somewhat destructive effect on the transmission through the system, as seen in Figure 9. The $\pi-\pi$ stacking is thus confirmed to be the significant interaction that allows for transmission through Di-Co^{2+}. We are considering the possibility of optimizing the transmission through the $\pi-\pi$ stacking interaction of monolayers by either a change of the structure of the organic ligands or the use of a different bridging ligand (such as Cl^-) or metal ion. An improved $\pi-\pi$ stacking interaction within the molecular device is expected to result in further amplified conductivity.

4. Conclusions

Computational models have been used to analyze measured conductance through a complex of cobalt(II) with terpyridine based SAMs formed *in situ*. We emphasize that the complexes formed *in situ* and *ex situ* are not guaranteed to be the same. We suggest, in fact, that the complex responsible for the conducting devices is different from that formed *ex situ*. The Mono-Co^{2+} [bis(Pt-S-ph-terpy)cobalt(2+)] complex is found to be the most stable under normal solution conditions. However, under the constraints imposed by the nanogaps, Di-Co^{2+} [bis-(μ-acetato-κ^2O,O′)-bis(Pt-S-ph-terpy-cobalt)(2+)], or a similar bridged (μ-type) complex, is more likely to form. This Di-Co^{2+} complex is both longer and more flexible than the Mono-Co^{2+} form, and, therefore, is more suited to span the fabricated nanogap as a molecular device.

It is shown that the Di-Co^{2+} structure exhibits more efficient electron transport than Mono-Co^{2+}. This is attributed to the nature of the π conjugated systems across the molecular wire. It is demonstrated that the acetate bridge between the two metal centers in the Di-Co^{2+} structure leads to a π system that is delocalized across the two organic ligands and that connects the two platinum leads. This delocalization allows for improved transmission through Di-Co^{2+} and is shown to be related to a limited π stacking interaction between the two organic ligands. The metal center in Mono-Co^{2+}, on the other hand, acts more as a tunnel barrier, where the two π systems of the organic ligands are oriented perpendicular to each other across the Co^{2+} bridge. In addition, our results suggest that further optimization of the conductance is achievable by modifying the bridging agent and/or the molecular socket as defined by the monolayers.

Acknowledgment. B.D.D. acknowledges Prof. Colin Nuckolls for useful and insightful discussions. We also acknowledge J. Brannon Gary for participating in some brainstorming discussions related to this research. B.D.D. acknowledges the University of Michigan and the Petroleum Research Fund of the American Chemical Society (through PRF Grant 47118-G6) for financial support. We acknowledge the National Energy Research Scientific Computing Center (NERSC) for awarding computing time.

Supporting Information Available: Coordinate (xyz) files of the optimized geometries of Mono-Co^{2+} and Di-Co^{2+} models are provided. This material is available free of charge via the Internet at http://pubs.acs.org.

References and Notes

(1) Tang, J.; Wang, Y.; Nuckolls, C.; Wind, S. J. *J. Vac. Sci. Technol. B* **2006**, *24*, 3227−3229.
(2) Tang, J. Y.; Wang, Y. L.; Klare, J. E.; Tulevski, G. S.; Wind, S. J.; Nuckolls, C. *Angew. Chem., Int. Ed.* **2007**, *46*, 3892−3895.
(3) Morgan, G.; Burstall, F. H. *J. Chem. Soc.* **1937**, *Part 2*, 1649−1655.
(4) Hogg, H.; Wilkins, R. G. *J. Chem. Soc.* **1962**, January, 341−350.
(5) Harris, C. M.; Lockyer, T. N.; Martin, R. L.; Patil, H. R. H.; Sinn, E.; Stewart, I. M. *Aust. J. Chem.* **1969**, *22*, 2105−2116.
(6) Andres, P. R.; Hofmeier, H.; Lohmeijer, B. G. G.; Schubert, U. S. *Synthesis* **2003**, *18*, 2865−2871.
(7) Holyer, R. H.; Hubbard, C. D.; Kettle, S. F. A.; Wilkins, R. G. *Inorg. Chem.* **1966**, *5*, 622−625.
(8) Prasad, J.; Peterson, N. C. *Inorg. Chem.* **1969**, *8*, 1622−1625.
(9) Judge, J. S.; Reiff, W. M.; Intille, G. M.; Ballway, P.; Baker, W. A., Jr. *J. Inorg. Nucl. Chem.* **1967**, *29*, 1711−1716.
(10) Constable, E. C.; Housecroft, C. E.; Jullien, V.; Neuberger, M.; Schaffner, S. *Inorg. Chem. Commun.* **2006**, *9*, 504−506.
(11) Park, J.; Pasupathy, A. N.; Goldsmith, J. I.; Chang, C.; Yalsh, Y.; Petta, J. R.; Rinkoski, M.; Sethna, J. P.; Abruña, H. D.; McEuen, P. L.; Ralph, D. C. *Nature* **2002**, *417*, 722−725.
(12) Shao, Y.; Molnar, L. F.; Jung, Y.; Kussmann, J.; Ochsenfeld, C.; Brown, S. T.; Gilbert, A. T. B.; Slipchenko, L. V.; Levchenko, S. V.; ONeill, D. P.; DiStasio, Jr. R. A.; Lochan, R. C.; Wang, T.; Beran, G. J. O.; Besley, N. A.; Herbert, J. M.; Lin, C. Y.; Van, Voorhis, T.; Chien, S. H.; Sodt, A.; Steele, R. P.; Rassolov, V. A.; Maslen, P. E.; Korambath, P. P.; Adamson,

R. D.; Austin, B.; Baker, J.; Byrd, E. F. C.; Dachsel, H.; Doerksen, R. J.; Dreuw, A.; Dunietz, B. D.; Dutoi, A. D.; Furlani, T. R.; Gwaltney, S. R.; Heyden, A.; Hirata, S.; Hsu, C.-P.; Kedziora, G.; Khalliulin, R. Z.; Klunzinger, P.; Lee, A. M.; Lee, M. S.; Liang, W. Z.; Lotan, I.; Nair, N.; Peters, B.; Proynov, E. I.; Pieniazek, P. A.; Rhee, Y. M.; Ritchie, J.; Rosta, E.; Sherrill, C. D.; Simmonett, A. C.; Subotnik, J. E.; Woodcock, H. L., III; Zhang, W.; Bell, A. T.; Chakraborty, A. K.; Chipman, D. M.; Keil, F. J.; Warshel, A.; Hehre, W. J.; Schaefer, H. F., III; Kong, J.; Krylov, A. I.; Gill, P. M. W.; Head-Gordon, M. *Phys. Chem. Chem. Phys.* **2006**, *27*, 3172−3191.

(13) Becke, A. D. *J. Chem. Phys.* **1993**, *98*, 1372−1377.

(14) Becke, A. D. *J. Chem. Phys.* **1993**, *98*, 5648−5652.

(15) Wadt, W. R.; Hay, P. J. *J. Chem. Phys.* **1985**, *82*, 299−310.

(16) Samanta, M. P.; Tian, W.; Datta, S.; Henderson, J. I.; Kubiak, C. P. *Phys. Rev. B* **1996**, *53*, R7626−R7629.

(17) Tian, W.; Datta, S.; Hong, S.; Reifenberger, R.; Henderson, J. I.; Kubiak, C. P. *J. Chem. Phys.* **1998**, *109*, 2874−2882.

(18) Mujica, V.; Nitzan, A.; Mao, Y.; Davis, W.; Kemp, M.; Roitberg, A.; Ratner, M. A. *Adv. Chem. Phys.* **1999**, *107*, 403−429.

(19) Xue, Y.; Datta, S.; Ratner, M. A. *J. Chem. Phys.* **2001**, *115*, 4292−4299.

(20) Baer, R.; Neuhauser, D. *J. Am. Chem. Soc.* **2002**, *124*, 4200−4201.

(21) Liu, C.; Walter, D.; Neuhauser, D.; Baer, R. *J. Am. Chem. Soc.* **2003**, *125*, 13936−13937.

(22) Yaliraki, S. N.; Roitberg, A. E.; Gonzalez, C.; Mujica, V.; Ratner, M. A. *J. Chem. Phys.* **1999**, *111*, 6997−7002.

(23) Landauer, R. *Philos. Mag.* **1970**, *21*, 863.

(24) Bagwell, P. F.; Orlando, T. P. *Phys. Rev. B* **1989**, *40*, 1456−1464.

(25) Imry, Y.; Landauer, R. *Rev. Mod. Phys.* **1999**, *71*, S306−S312.

(26) López-Sancho, M. P.; López-Sancho, J. M.; Rubio, J. *J. Phys. F: Met. Phys.* **1985**, *15*, 851−858.

(27) Nardelli, M. B. *Phys. Rev. B* **1999**, *60*, 7828−7833.

(28) Coordinate (xyz) files of the optimized geometries of Mono-Co^{2+} and Di-Co^{2+} models are available as Supporting Information.

(29) Hutchinson, G. R.; Ratner, M. A.; Marks, T. J. *J. Am. Chem. Soc.* **2005**, *127*, 16866−16881.

(30) Chen, Y. C.; Prociuk, A.; Perrine, T. M.; Dunietz, B. D. *Phys. Rev. B* **2007**, *74*, 245320.

(31) Perrine, T. M.; Dunietz, B. D. *Nanotechnology* **2007**, *18*, 424003.

(32) Xiao, X.; Xu, B.; Tao. N. J. *Angew. Chem., Int. Ed.* **2004**, *43*, 6148.